Journal of Micromechanics and Microengineering

PAPER • **OPEN ACCESS**

Rotational UV-lithography using flexible chromium-coated polymer masks for the fabrication of microstructured dental implant surfaces: a proof of concept

OPEN ACCESS
IOP Publishing
Journal of Micromechanics and Microengineering
J. Micromech. Microeng. **30** (2020) 045008 (9pp)
https://doi.org/10.1088/1361-6439/ab70c0

Rotational UV-lithography using flexible chromium-coated polymer masks for the fabrication of microstructured dental implant surfaces: a proof of concept

P W Doll[1], C Doll[2], L Käßer[1], M Häfner[1], B Spindler[3], R Ahrens[1], S Nahles[2], M Heiland[2] and A E Guber[1]

[1] Karlsruhe Institute of Technology, Institute of Microstructure Technology, Hermann-von-Helmholtz-Platz 1, 76344 Eggenstein-Leopoldshafen, Germany
[2] Department of Oral and Maxillofacial Surgery, Charité—Universitätsmedizin Berlin, Corporate Member of Freie Universität Berlin, Humboldt-Universität zu Berlin, Berlin Institute of Health, Berlin, Germany
[3] Fräszentrum Ortenau GmbH & Co KG, Industriestr. 2-4, 77728 Oppenau, Germany

E-mail: patrick.doll@kit.edu

Received 17 September 2019, revised 13 January 2020
Accepted for publication 28 January 2020
Published 25 February 2020

Abstract

The purpose of this work was to demonstrate the technical feasibility for the fabrication of microgrooves or micropits on dental implants or dental implant abutment surfaces using a novel fabrication method derived from common UV-lithographic microfabrication. Instead of using a flat and rigid chromium/glass mask to structure a photoresist layer on a small cylindrical part, a flexible chromium-coated polymer mask was introduced into the lithographic setup. Through an elastic deformation of the polymer mask, it was possible to achieve lateral resolutions as small as 1.5 μm on small cylinders and to structure conical parts. By subsequent controlled under-etching of the structured photoresist layer, microgrooves of different cross-sectional geometries can be generated and applied to the implant or implant abutment surface. Such structures can be used for contact guidance of human gingival fibroblasts or endothelia cells to enhance the wound healing process and the overall soft-tissue integration.

Keywords: rotational lithography, microgrooves, soft-tissue integration, dental implants

(Some figures may appear in colour only in the online journal)

1. Introduction

Nowadays, the placement of dental implants is considered a routine procedure for the rehabilitation of fully or partially edentulous patients [1]. Besides the osseointegration of the implant body, (long-term) success depends on the integration of the implant abutment interface with the patient's soft tissue, so that it can establish a biological barrier against the oral cavity [2, 3] for example, preventing epithelial down growth with peri-implant bone loss caused by bacterial colonization [4].

The physical or chemical modification of titanium can improve peri-implant soft-tissue attachment [5, 6]. It has been shown that microgrooves applied to the implant titanium surface can guide the cells towards the desired direction to speed up and enhance soft-tissue integration [7–10]. The manufacturing of such structures is often carried out using laser ablation technique [11–15]. An ultrashort pulse laser, such as a femtosecond laser, is used to melt down and vaporize the material locally. In principle, various microtextures and

microgrooves can be generated; to date, typically 20 μm microgrooves have been produced. However, the surface was not treated any further, so local heat-affected zones overlaid the material, altering the physical and chemical properties of the surface of the grooves [13]. The overall cross-sectional geometry of the grooves mainly depends on the properties of the laser ablation technique such as the speed and power of the laser [11–15]. In addition, the cross-sectional geometries of the grooves are limited by the principle of the laser ablation setup.

Besides the laser ablation technique, another fabrication method is electrochemical discharge micromachining, where an electrode is used to electro-chemically erode the material locally [16, 17]. The electrode can have different shapes. In the case of wire erosion, a small wire electrode is used to cut the material [17]. Although the method itself is a good way to create microgrooves, the treatment and removal of the heat-affected zones and material impurities due to the chemical reaction with the electrolyte used, limits the minimum lateral resolution and overall quality of the method, yet the smallest width reported was 20 μm [17]. Another fabrication method is micromachining where small tools, such as cemented carbide tools, are used to cut into the material [18]. This fabrication method is of course highly limited due to the available size of the tools.

As a different approach for structuring commercially pure titanium (cpTi) or the alloy titanium Gr. 5 ELI (Ti6Al4V ELI) to create microgrooves, we have tested the suitability of a lithographic-based manufacturing process in combination with wet etching. Lithography is well known in microtechnology and is mainly used to structure silicon-based substrates [7, 19, 20]. The anisotropic etching of silicon with, for example, potassium hydroxide results in typical rectangular or triangular profiles due to the crystallographic orientation of the substrate.

In the case of titanium or titanium alloys, the etching with hydrofluoric acid (HF) is isotropic [21]. In contrast to silicon etching, sharp edges (rectangles or triangles) are not possible due to the isotropic nature of the etch process. However, by controlled under-etching of the lithographically applied mask, different cross-sections of the grooves are possible [21]. These cross-sectional geometries can range from slightly rectangular over smoothed rectangular structures, curvy/spiked to sinus-shaped profile geometries. These different kinds of profiles have not yet been used for contact guidance experiments nor has the fabrication method for various cross-sectional geometries been reported for cylindrical or conical titanium parts, which are used for dental implants or implant abutments.

The aim of the present work is to demonstrate a novel and patented method for the fabrication of microgrooves or micropits on such small cylindrical parts. These kinds of structures can be applied to dental implants or implant abutments for the so-called contact guidance of human gingival fibroblasts or endothelial cells to enhance the wound healing process and the overall soft-tissue integration of the implant.

2. Material and methods

2.1. Rotational UV-lithography using flexible chromium-coated polymer masks

Common mask-based UV lithography uses planar and rigid glass masks with reflective chromium structures on top, which are projected on a photoresist layer on a flat substrate (e.g. silicon or titanium) [21]. By exposure to UV radiation the structures of the mask are copied to the photoresist on top of the part by simple shadow projection. Depending on the tone of the resist used, the exposed or unexposed areas can then be developed with suitable chemicals [21]. An etching of the now uncovered areas will copy the structures into the substrate material. A subsequent stripping of the remaining resist will remove it, leaving only the structured substrate.

In principle, this procedure can also be carried out for cylindrical substrates such as dental implants. Yet, in the case of such cylindrical substrates the projection of a rigid glass mask is limited to a very small spot (line) on top of the sample due to the curved surface of the cylinder (compare figure 1). To avoid mask damage, it is normally placed slightly above the sample with a small distance (proximity) between the mask and sample surface (e.g. 20 μm).

Only a few studies have shown that it is basically possible to work with planar masks in a proximity exposure setup to lithographically structure small (and large) cylinders [22, 23]. The smallest lateral structure width achieved on small cylinders was 5 μm [22]. The experimental setup was complex and the necessary quality of the cylinders (e.g. roundness error) was high, which makes the method more expensive. Conical parts could not yet be structured.

If instead of a rigid and planar glass mask a flexible mask made of polymer is introduced into the lithographic setup, this mask can adapt to the radial shape of the part due to a small elastic deformation, when it is pulled towards the sample, as shown in figure 1. The deformation will result in a surface contact between the mask and part, which increases the available area for a precise projection of the mask and minimizes the proximity between the mask and part.

2.2. Mask design

As carrier material for the reflective chromium coating, 80 μm thick cycloid olefin copolymer (COC) foils (TOPAS® 8007F-04, TOPAS Advanced Polymers GmbH, Germany) were used. In general, every polymer foil should be usable, even a very thin glass layer, as long as they are flexible enough to adapt to the radial shape of the part and are resistant to the cleaning and development chemicals. The foil sheet was first cut into approx. $50 \times 50\,\text{mm}^2$ pieces. The separate pieces were cleaned by successive dipping and rinsing with acetone, isopropanol (IPA) and deionized (DI) water and dried with compressed nitrogen. The cleaned foils were each placed on a 4″ silicon wafer and a 10 min oxygen plasma ($R_F = 100$ W,

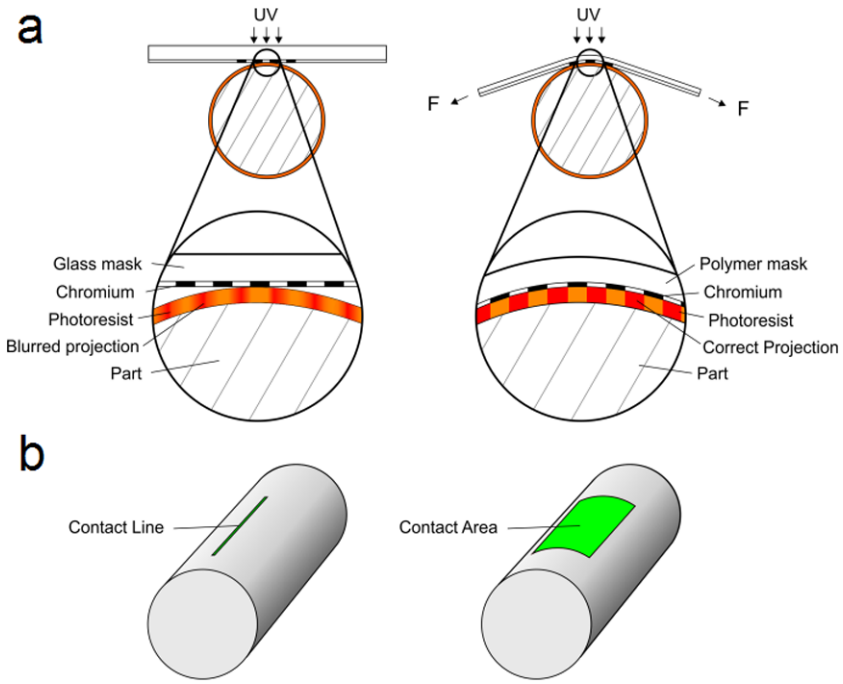

Figure 1. (a) Comparison of common lithography technique (left) using a rigid glass mask and flexible mask (right). By using a flexible mask, the projection can be accurate instead of blurred due to diffraction, as a result of proximity effects between the mask and resist. (b) Schematic drawing of the contact area of a rigid glass mask (left) and a flexible mask (right). Resulting area is exaggerated and just for general comprehension purposes only. Sizes are not to scale.

50 sccm O_2) for further cleaning, and conditioning was performed before chromium coating.

The foils were then coated with a 100 nm chromium layer by electron beam vapor deposition (UVEX 400, Leybold GmbH, Germany).

After chromium deposition, the foils were coated with a positive tone photoresist (AZ1505, Merck Performance Materials, Germany) by spin coating (60 s at 1000 rpm, acceleration ramp of 1500 rpm s^{-1}). The coating procedure results in an average resist thickness of approx. 1 ± 0.1 μm.

A common commercially available 5″ chromium glass mask (DeltaMask B.V, Netherlands) was then lithographically copied to the resist layer on top of the polymer foils. The glass mask used consists of various fields containing different structures such as lines with various lateral sizes, dot arrays with varying diameters and distances, etc. For one flexible mask, only one of these small fields is used and necessary. Thereby, many different masks can be produced at once on a single $50 \times 50\,mm^2$ foil. The exposure was carried out using a flood exposure system with a peak wavelength at 405 nm (LH5, Suss Microtec AG, Germany) at a dose of 100 mJ cm^{-2}.

After exposure, the samples were developed in a mixture of AZ400K (Merck, Performance Materials GmbH, Germany) and DI water (1:4) for 60 s, to remove the exposed areas.

The now uncovered areas were etched using chromium etchant (TechniEtch Cr01, MicroChemicals GmbH, Germany) for 30 s. After etching, the remaining photoresist was stripped off using acetone and the foils were cleaned by rinsing with IPA and DI water.

Each mask field was then cut out and fixed onto a prepared polyimide carrier foil. This foil had a cut-out window where the structured COC foil was placed, so the UV radiation only passes this area. This mask assembly was then clamped into the setup's mask-holding mechanism (see figure 2).

2.3. Experimental setup

Rotational lithography requires a relative rotational movement between the part and mask. In our setup, the part rotates while the mask stays still.

Before the mask is applied to the part, it is moveable in *x*, *y* and *r*-directions (compare figure 2(a)), allowing precise placement onto the part. Right before exposure, the mask is clamped (vertical direction) onto the part, creating a tight contact between the mask and part.

To be able to rotate the part and control the velocity, a stepper motor setup with an additional geared belt drive with a reduction of 1:3.25 was used. To avoid eccentric movement of the part, a special adapter (ER16 clamp tool) was used. The setup is operated by a microcontroller setup and controlled via a 3.2″ touch screen. The mask is applied to the part using a special holder via springs on one side.

2.4. Sample material

Since titanium is mostly used for dental implants as well as other medical implants, we demonstrate the technique on this material. To further demonstrate the possibilities of the

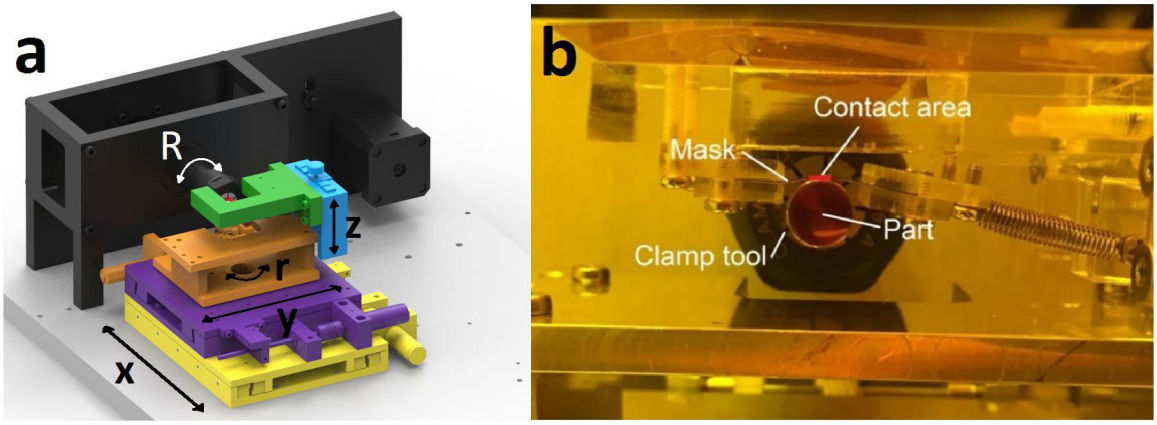

Figure 2. (a) Schematic overview of the experimental setup showing the components of the setup and available axes for mask alignment. Black: motor, gear, *r*-axis and clamp tool; yellow: *x*-axis, purple: *y*-axis, blue: *z*-axis; orange: *r*-axis; green: mask holder. Housing, control unit, shutter and UV-lamp are not displayed for better visualization (b) detail photograph of the experimental rotational exposure setup. Part is clamped centrically by an ER16 clamp tool. Mask is applied to the part over a special mask holder, which is movable in *x*, *y*, *z* and *r*-directions. Via *z*-movement of the holder and the connected springs, it is applied to the part creating a close contact area for exposure.

technique to structure different materials, we also show the microstructuring of polyether ether ketone (PEEK) substrates (PEEK rod, 8 × 1000 mm, Merz Dental GmbH, Germany).

The titanium and PEEK samples were first cut into 30 mm long cylinders and cleaned with acetone, IPA and DI water. A subset of samples was put aside and the surface was left as received. Samples of each material were ground using different silicon carbide (SiC) grinding paper (P400-P2500; Struers GmbH, Germany). To recognize individual samples, one side of each sample was uniquely marked containing the batch and sample number by a laser marking system. To achieve an adequately flat surface finish for the UV-lithography process, the samples were finally polished using a 9 μm diamond suspension (DiaDuo-2, Struers GmbH, Germany). After sample preparation, all samples were cleaned in an ultrasonic bath for 10 min with IPA and DI water, respectively, and dried with compressed nitrogen.

2.5. Coating and softbake

As photoresists, positive tone photoresists (AZ4533 and AZ1505, Merck Performance Materials GmbH, Germany) and one negative tone photoresist (SU-8 3005, MicroChem Corp, USA) were tested.

To evenly coat the cylinders with an adequately thin resist layer, the process of dip coating can be used [24]. The samples are immersed in the photoresist and slowly pulled out. The resulting layer thickness mainly depends on the viscosity of the photoresist and the retraction speed [24].

For the dip-coating procedure, a computer-controlled precision linear stage (LTM80, Owis GmbH, Germany), which ensures high precision and jitter-free movement was used. The coating programme consists of the immersion of the sample in the resist, a holding period of 30 s (dwell time) and the retraction of the sample, where it is slowly extracted with a defined speed (2–10 mm min^{-1}).

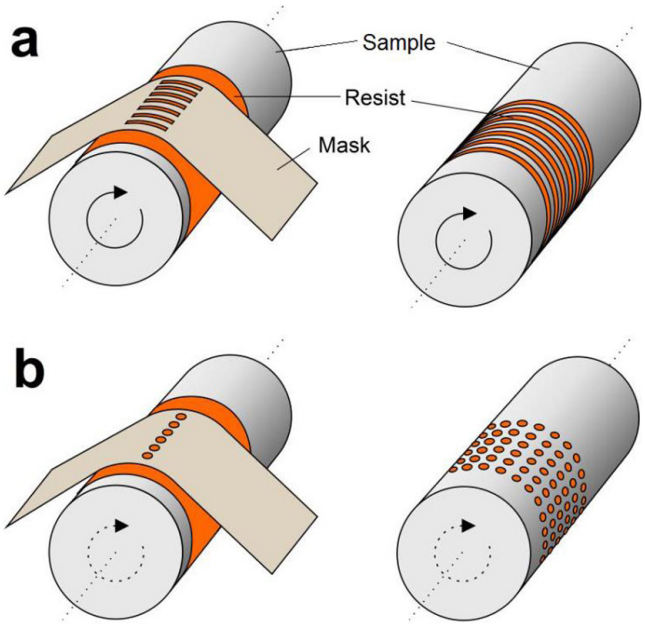

Figure 3. Schematic drawing of the exposure setup and possible structures. Mask is in close contact with the resist on top of the part. Part rotates continuously (a) or stepwise (b) while exposed to adequate radiation. In the case of continuous movement of the part (a) the exposed structures are closed loop patterns while for a stepwise exposure (b) single elements like circles can be generated.

Directly after coating, the samples were turned over and placed in an oven for 1 h at 95 °C to remove the remaining solvent (softbake).

2.6. Rotational exposure

A schematic drawing of the exposure setup is shown in figure 3. By controlling the rotation speed, rotation angle, exposure time, etc, the system is fully adjustable to fabricate a broad variety of microstructures from revolving microgrooves

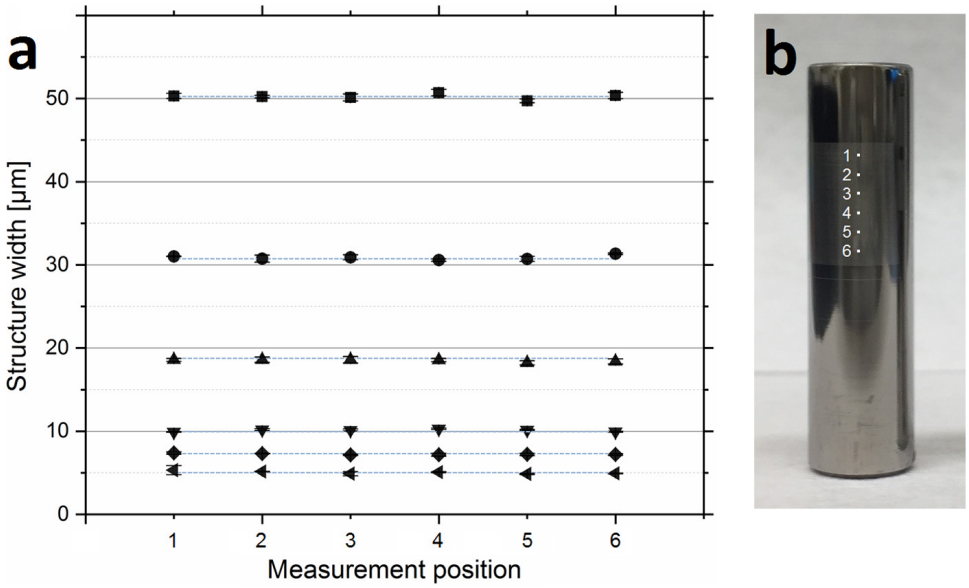

Figure 4. (a) Results of microscopic mask inspection after lithography and development for different lateral structure widths. Along the structured area, six individual measurement positions have been analysed. Dotted blue lines indicate the structure widths of the original mask. (b) Image of a lithographically structured sample of 8 mm diameter and indication of measurement positions.

to single elements such as pits or pillars. Since no UV-light source is integrated into the exposure setup, a UV-light flood exposure system (LH5, Süss Microtec AG, Germany) was used to expose the samples. The exposure time is set by an optical shutter, which was also controlled by the microcontroller setup.

For continuous movement to produce revolving microgrooves, the shutter was opened at the beginning of the exposure and stayed open while the part is rotated and exposed and was closed after finishing the movement. The rotation speed is determined by the necessary dose for complete exposure of the photoresist, the circumference of the part and number of rotations.

To expose single elements, a stepwise movement and exposure are necessary. For this, the shutter opens for exposure while the sample is held in a fixed position. After the necessary time for full exposure, the shutter is closed again and the part is rotated to the next feature and so on.

The intensities used for exposure are 120 mJ cm^{-2} for AZ4533, 100 mJ cm^{-2} for AZ1505 and for SU-8 3005 150 mJ cm^{-2}.

2.7. Development

After exposure, the samples were manually developed in a mixture of AZ400K Developer and DI water (1:4) for 120 s for AZ4533 and 60 s for AZ1505, respectively. For SU8, the development was carried out in propylene glycol monomethyl ether acetate (PGMEA, MicroChemicals GmbH, Germany) for 1 h.

2.8. Wet etching

To copy the structured resist pattern into the substrates and to form different microgroove cross-sectional geometries or micropits, the titanium samples were wet etched for various times from a few seconds to several minutes, depending on the photoresist pattern sizes and the desired cross-sectional geometry form. As etchant, a mixture of hydrofluoric acid (5%) (BASF, Germany), hydrogen peroxide (31%) (BASF, Germany) and DI water (11 HF: 1 H_2O_2: 10 H_2O) was used.

After the etching procedure, the samples were cleaned in a DI water bath and dried with compressed nitrogen. The remaining photoresist was stripped off using acetone for 30 s. Afterwards, the samples were cleaned by rinsing with IPA followed by DI water and dried with compressed nitrogen. After removing the photoresist, a short second etch step can be performed to remove the polished surface to get a homogenous surface structure. The etching can be performed using the same etchant and conditions, but just for a few seconds, thus removing only a very small amount of the material.

3. Results

3.1. Revolving microgrooves

For the use as dental implants or dental implant abutment surfaces, samples with different diameters have been structured with revolving microgrooves of different lateral widths. The method has been successfully used on samples with diameters of 8, 5, 3 and 2.5 mm with 2.5 mm being the smallest available diameters of the samples. In principle, the rotational lithographic setup also allows structuring of samples with smaller diameters.

The resulting depiction quality was analyzed using optical microscopy with a magnification of 100×, 250× or 500×, depending on the lateral structure width of the mask. For widths smaller than at least 50 μm, triplicates were fabricated and analyzed. The results of this analysis for revolving structures are shown in figure 4. The overall depiction quality is

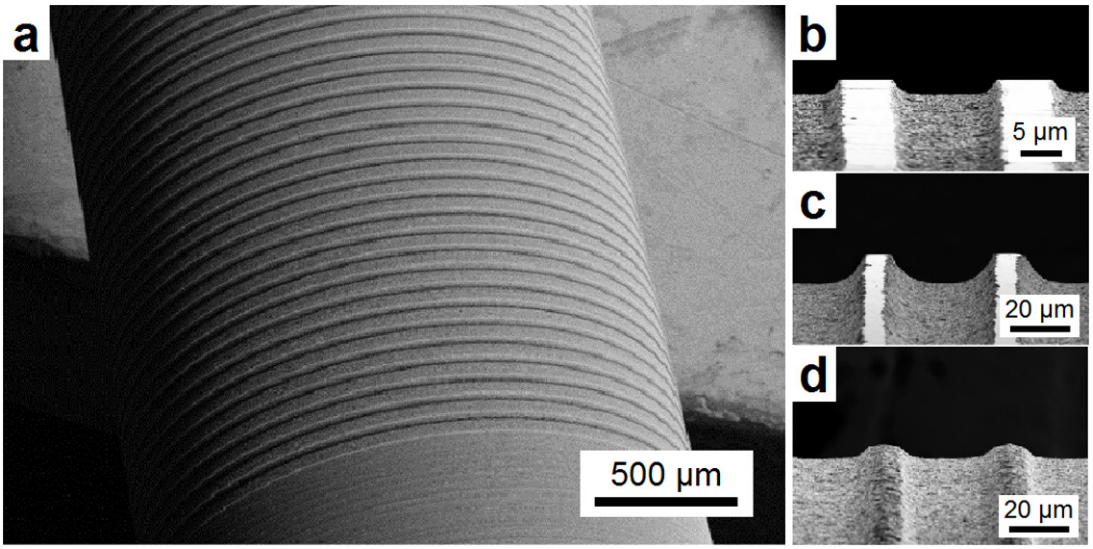

Figure 5. Scanning electron micrographs of test samples. (a) Titanium sample with a diameter of 3 mm structured with 50 μm wide revolving microgrooves. (b)–(d) Different cross-sectional geometries that can be generated by controlled under-etching of the lithographically structured photoresist. (b) Squared microgrooves; (c) spiky/U-shaped microgrooves; (d) sinusoidal microgrooves.

comparable to common glass mask-based lithographic depiction. On average, an error smaller than ± 0.4 μm could be achieved, allowing precise and reproducible microstructuring. The smallest possible structure width successfully copied into the resist layer while constantly rotating the sample, was a lateral width of 5 μm. Below that, the effect of movement combined with the surface roughness and roundness errors of the samples only allowed partially accurate structuring.

Figure 5(a) shows a scanning electron micrograph of a titanium cylinder with a diameter of 2.5 mm and revolving microgrooves of a 50 μm widths, which have been wet etched into the cylinder. As can be seen, the microgrooves can be evenly applied to the titanium cylinder without any errors. One big advantage of the fabrication method is the possibility to realize different cross-sectional geometries, which can be achieved by controlled under-etching of the lithographically applied and structured photoresist layer [21]. The resulting cross-sections are a consequence of mask setup (lateral structure width, ridge/gap ratio) and etching time. Figures 5(b)–(d) show scanning electron micrographs of differently treated titanium samples to achieve different cross-sectional geometries by controlled under-etching of the lithographically applied and structured photoresist layer. In this case, a mask was used with a ridge-to-groove ratio (duty cycle) of 1:1. By changing this ratio, the ridges and groove sizes can be altered and together with a defined etching time (see equation (2)) a broad variety of different possible surface structures can be fabricated [21].

3.2. Single elements

Besides completely revolving elements such as microgrooves, single elements such as micropits have been created. In this case, the rotation and exposure of the substrate were carried out stepwise.

The smallest structures in our experiments that could be successfully copied had diameters of 1.5 μm, which represents the smallest available spot size on the commercially available chromium/glass mask.

To our knowledge, this is to date the smallest lithographically copied structure that has been applied to cylinders with diameters as small as 8 mm or even 2.5 mm. Figure 6 shows scanning electron micrographs of different single elements on PEEK and titanium samples. Figure 6(a) shows 50 μm circles, which have been copied into the photoresist layer on top of an untreated (as received) PEEK cylinder with a diameter of 8 mm. Figure 6(b) shows the corresponding detail of figure 6(a). Figure 6(c) shows the surface of a structured titanium sample showing approx. 7.5 μm holes, which have been etched into the titanium material using a 5 μm circular pattern arrangement. Figure 6(d) shows the detail of figures 6(c) and (e) shows the surface of a structured titanium sample showing approx. 2.5 μm holes, which have been etched into the material using a 1.5 μm circular pattern arrangement.

In contrast to revolving microgrooves, the factor of movement was not found to be critical for single features. The overall structuring of single elements could be performed much more stably compared to the fabrication of revolving microgrooves, since there is no motion of the sample during the exposure.

4. Discussion

The presented fabrication method allows the precise structuring of small cylindrical parts such as dental implants or dental implant abutments by UV-lithographic microfabrication. Instead of using a flat and rigid chromium/glass mask to structure a photoresist layer on a small cylindrical part, for the first time we introduced a flexible chromium-coated

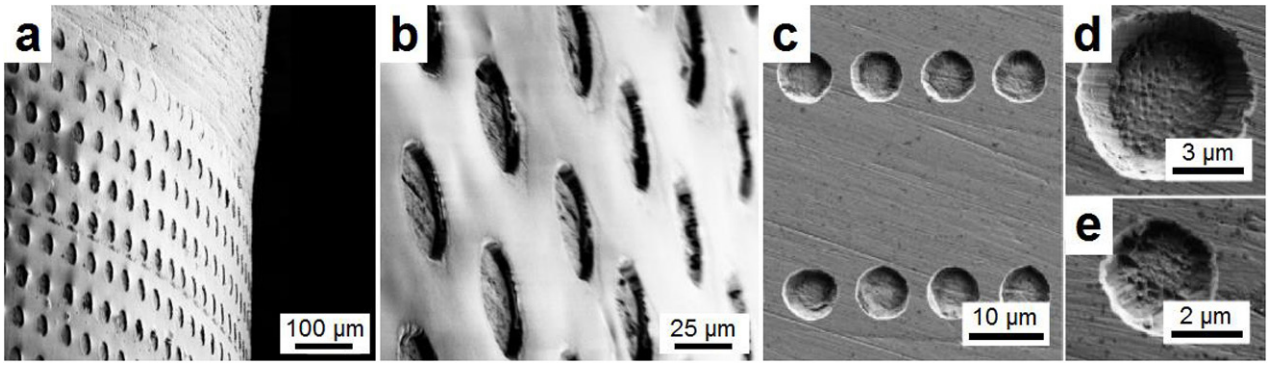

Figure 6. Scanning electron micrographs of PEEK and titanium samples with diameters of 8 mm, which were lithographically structured by rotationally lithography. (a) As-received PEEK sample covered with 50 μm circular holes in the resist layer and the detail (b). (c) Surface of a structured titanium sample showing approx. 7.5 μm holes, which have been etched into the material using a 5 μm circular pattern and the detail (d). (e) Surface of a structured titanium sample showing approx. 2.5 μm holes, which have been etched into the material using a 1.5 μm circular pattern.

polymer mask into the lithographic setup. Through an elastic deformation of the polymer mask when it is slightly pulled towards the cylindrical sample, it is possible to avoid resolution-limiting diffraction by creating a tight contact between the mask and part, realizing a contact exposure setup. This proximity-free exposure realizes minimal lateral resolutions for single elements as small as 1.5 μm, which is near the common mask-based, wavelength-dependent resolution limit. To achieve such small lateral features, the overall surface roughness plays a crucial role in UV-lithographic microfabrication. While lateral feature widths of $\geqslant$10 μm could be realized on the 'as-received' samples with no further surface treatment ($R_a = 160$ nm) (compare figure 6(a)), an adequate flat surface is mandatory for smaller lateral structures, especially if the structures are smaller than 5 μm. If the surface roughness is too high, the distances between higher and lower features of the surface topography result in different distances between the mask and part, which results in diffraction and blurred projections, respectively. If the sample surface is adequately prepared (polished or electropolished) and has a smooth surface roughness (e.g. smaller than a few nm) and also only a small waviness, smaller lateral feature sizes can be easily realized. Within this work we were able to achieve the full UV-lithographic resolution with feature sizes of approx. 1.5 μm to small titanium cylinders. The lateral sizes were the smallest sizes available on a commercially available chromium/glass photomask, which was used for the fabrication of the flexible chromium-coated polymer mask. Slightly smaller lateral structure widths might also be possible, depending on the wavelength used for exposure and the thickness of the resist, which is applied to the sample.

Besides the better resolution in contrast to a lithographic setup using a rigid glass mask, the use of a flexible chromium-coated polymer mask provides another benefit when it comes to roundness errors of the samples. Such an error will result in different proximities between the mask and part for a setup using a glass mask and proximity exposure while the part rotates. In the setup, using a flexible polymer mask, a roundness error of the part is automatically compensated by the experimental design, since the mask is pulled towards the sample, which is in close contact with it and adapts to its shape (compare figure 2). This contact exposure realizing the small possible feature sizes is yet one main drawback of the presented fabrication method since it results in wear of the mask and thus limited lifetime of the mask compared to a proximity exposure setup where a distance between mask and sample is present and the mask is not damaged due to wear. In our experiments, a single mask could be used at least five times on a sample with a diameter of 8 mm until the first signs of mask damage could be recognized from the resulting projections. In this case, parts of single chromium lines from the line patterns were broken or missing when the masks were inspected after exposure. Although this damage occurs, it can be neglected for scientific and especially industrial manufacturing, since the mask itself can easily be fabricated and replaced. As described earlier, within one batch of fabrication a large number of individual masks can be generated at once. For industrial application, a roll-to-roll principle should be applied where a coupling of the mask movement and the rotation of the sample can also be realized. Introducing such a setup will also enable the projection of arbitrary patterns with more complete geometries and further applications such as stents can be addressed [25]. In addition, grid patterns should also be generated to demonstrate further capabilities of the fabrication method.

The resulting microgrooves after wet etching (figure 5) can be generated precisely and are reproducible. The wet etching of the material will result in higher surface roughness values than the roughness at the beginning of the process. This resulting surface roughness is mainly determined by the etchant used and grain size of the material. The isotropic etching of titanium and its alloys can be performed very accurately, resulting in reproducible surface structuring and corresponding cross-sectional geometries, yet the experimental setup (etchant mixture, stirring etc) must be controlled strictly.

5. Conclusions

Within this work, we could demonstrate for the first time a rotational UV-lithographic approach using flexible chromium-coated polymer masks to structure small cylindrical parts. Titanium and PEEK samples could successfully be structured and covered with revolving microgrooves or single elements such as micropits.

By using flexible chromium-coated polymer masks, which can be elastically deformed to adapt the radial shapes of the parts, microstructures down to lateral sizes of 1.5 μm have been created. By continuously exposing the photoresist on the parts through the applied mask while rotating the part, revolving microstructures can be fabricated. By subsequent under-etching of the lithographically structured photoresist layer, different cross-sectional geometries of the microgrooves could be realized. Such grooves placed on the neck of dental implants or dental implant abutments can have significant positive effects for the attachment strength of the surrounding soft tissue and the overall soft-tissue integration of the implant system. Besides microgrooves, single elements such as pits or pillars can be fabricated if the samples are exposed stepwise.

The minimal lateral feature sizes possible and the variety of different cross-sectional geometries that can be realized with the presented method are major benefits compared to state-of-the-art mechanical microfabrication methods or even laser ablation.

The presented method will enable a variety of new developments, especially in medical microtechnology where curved or cylindrical substrates are used, highest precision is necessary and small lateral resolutions are required.

Acknowledgments

This work was supported by the German Federal Ministry for Economic Affairs and Energy (BMWi) (Grant No: KF2308206KJ4).

The authors thank B Hübner and Dr U Köhler for their help with wet etching.

Disclosures

The authors PWD, LK, RA and AEG applied for a patent of the presented fabrication method (DE102017121097A1). MH, CD, BS, SN and MH declare no conflict of interest.

ORCID iDs

P W Doll https://orcid.org/0000-0001-9198-2756

References

[1] Bosshardt D D, Chappuis V and Buser D 2000 Osseointegration of titanium, titanium alloy and zirconia dental implants: current knowledge and open questions *Periodontology* **73** 22–40

[2] Rompen E, Domken O, Degidi M, Farias Pontes A E and Piattelli A 2006 The effect of material characteristics, of surface topography and of implant components and connections on soft tissue integration: a literature review *Clin. Oral Imp. Res.* **17** 55–67

[3] Gómez-Florit M, Ramis J M, Xing R, Taxt-Lamolle S, Haugen H J, Lyngstadaas S P and Monjo M 2014 Differential response of human gingival fibroblasts to titanium- and titanium-zirconium-modified surfaces *J. Periodont. Res.* **49** 425–36

[4] Iglhaut G, Schwarz F, Winter R R, Mihatovic I, Stimmelmayr M and Schliephake H 2014 Epithelial attachment and downgrowth on dental implant abutments—a comprehensive review *J. Esthet. Restor. Dent.* **26** 324–31

[5] Huh J-B, Rheu G-B, Kim Y-S, Jeong C-M, Lee J-Y and Shin S-W 2014 Influence of implant transmucosal design on early peri-implant tissue responses in beagle dogs *Clin. Oral Imp. Res.* **25** 962–8

[6] Al Rezk F, Trimpou G, Lauer H-C, Weigl P and Krockow N 2018 Response of soft tissue to different abutment materials with different surface topographies: a review of the literature *Gen. Dentist.* **66** 18–25

[7] Brunette D M 1986 Fibroblasts on micromachined substrata orient hierarchically to grooves of different dimensions *Exp. Cell Res.* **164** 11–26

[8] Lee H-J, Lee J, Lee J-T, Hong J-S, Lim B-S, Park H-J, Kim Y-K and Kim T-I 2015 Microgrooves on titanium surface affect peri-implant cell adhesion and soft tissue sealing; an *in vitro* and *in vivo* study *J. Periodont. Imp. Sci.* **45** 120–6

[9] Biela S A, Su Y, Spatz J P and Kemkemer R 2009 Different sensitivity of human endothelial cells, smooth muscle cells and fibroblasts to topography in the nano-micro range *Acta Biomater.* **5** 2460–6

[10] Lee S-W, Kim S-Y, Lee M-H, Lee K-W, Leesungbok R and Oh N 2009 Influence of etched microgrooves of uniform dimension on *in vitro* responses of human gingival fibroblasts *Clin. Oral Imp. Res.* **20** 458–66

[11] Vorobyev A Y and Guo C 2007 Femtosecond laser structuring of titanium implants *Appl. Surf. Sci.* **253** 7272–80

[12] Oliveira V, Ausset S and Vilar R 2009 Surface micro/nanostructuring of titanium under stationary and non-stationary femtosecond laser irradiation *Appl. Surf. Sci.* **255** 7556–60

[13] Fasasi A Y, Mwenifumbo S, Rahbar N, Chen J, Li M, Beye A C, Arnold C B and Soboyejo W O 2009 Nano-second UV laser processed micro-grooves on Ti_6Al_4V for biomedical applications *Mater. Sci. Eng.* C **29** 5–13

[14] Mukherjee S, Dhara S and Saha P 2015 Enhancing the biocompatibility of Ti6Al4V implants by laser surface microtexturing: an *in vitro* study *Int. J. Adv. Manuf. Technol.* **76** 5–15

[15] Dumas V, Rattner A, Vico L, Audouard E, Dumas J C, Naisson P and Bertrand P 2012 Multiscale grooved titanium processed with femtosecond laser influences mesenchymal stem cell morphology, adhesion, and matrix organization *J. Biomed. Mater. Res.* A **100** 3108–16

[16] Rathod V, Doloi B and Bhattacharyya B 2018 Machining guidelines for fabricating microgrooves of varied cross sections by electrochemical micromachining *Precision Product-Process Design and Optimization* ed S S Pande and U S Dixit (Berlin: Springer) pp 211–38

[17] Zhu D, Wang K and Qu N S 2007 Micro wire electrochemical cutting by using *in situ* fabricated wire electrode *CIRP Ann.* **56** 241–4

[18] Yang Y, Su Y, Li L, He N and Zhao W 2015 Performance of cemented carbide tools with microgrooves in Ti-6Al-4V titanium alloy cutting *Int. J. Adv. Manuf. Technol.* **76** 1731–8

[19] den Braber E, Deruijter J, Ginsel L, Vonrecum A and Jansen J 1996 Quantitative analysis of fibroblast morphology on microgrooved surfaces with various groove and ridge dimensions *Biomaterials* **17** 2037–44

[20] Doll P W, Al-Ahmad A, Bacher A, Muslija A, Thelen R, Hahn L, Ahrens R, Spindler B and Guber A E 2019 Fabrication of silicon nanopillar arrays by electron beam lithography and reactive ion etching for advanced bacterial adhesion studies *Mater. Res. Express* **6** 65402

[21] Doll P W, Semperowitsch C, Häfner M, Ahrens R, Spindler B and Guber A E 2018 Fabrication of micro structured dental implant abutments for optimized soft tissue integration *Curr. Direct. Biomed. Eng.* **4** 677–80

[22] Lima de Miranda R, Zamponi C and Quandt E 2009 Rotational UV lithography device for cylindrical substrate exposure *Rev. Sci. Instrum.* **80** 15103

[23] Chen H-W, Lee Y-C and Hsiao F-B 2010 Fabrication of seamless patterns onto metal rollers by photolithography *2010 IEEE 5th Int. Conf. on Nano/Micro Engineered and Molecular Systems* (*20–23 January 2010)* (Xiamen: IEEE) pp 887–92

[24] Giaconia C G, Grasso G and Arnone C 1995 Resist coating of cylindrical samples for 3D lithography *Microelectron. Int.* **12** 22–4

[25] Lima de Miranda R, Zamponi C and Quandt E 2009 Fabrication of TiNi thin film stents *Smart Mater. Struct.* **18** 104010